

# High speed interferometric ellipsometer

Chien-Chung Tsai,<sup>1,2+</sup> Hsiang-Chun Wei,<sup>1,2+</sup> Sheng-Lung Huang,<sup>2</sup> Chu-En Lin,<sup>3</sup>  
Chih-Jen Yu,<sup>3</sup> and Chien Chou,<sup>1,3,4,\*</sup>

<sup>1</sup>*Institute of Biophotonics, National Yang Ming University,  
Taipei, Taiwan 112*

<sup>2</sup>*Graduate Institute of Photonics and Optoelectronics and Department of Electrical Engineering, National Taiwan  
University, Taipei, Taiwan 106*

<sup>3</sup>*Department of Optics and Photonics, National Central University,  
Jhongli, Taiwan 320*

<sup>4</sup>*Department of Biomedical Imaging and Radiological Science, National Yang Ming University,  
Taipei, Taiwan 112*

\*Corresponding author: [cchou@ym.edu.tw](mailto:cchou@ym.edu.tw)

**Abstract:** A novel high speed interferometric ellipsometer (HSIE) is proposed and demonstrated. It is based on a novel differential-phase decoder which is able to convert the phase modulation into amplitude modulation in a polarized heterodyne interferometer. Not only high detection sensitivity but also fast response ability on ellipsometric parameters (EP) measurements based on amplitude-sensitive method is constructed whereas different amplitudes with respect to P and S polarized heterodyne signals in this phase to amplitude modulation conversion is discussed. The ability of HSIE was verified by testing a quarter wave plate while a real time differential-phase detection of a liquid crystal device versus applied voltage by using HSIE was demonstrated too. These results confirm that HSIE is able to characterize the optical property of specimen in terms of EP at high speed and high detection sensitivity experimentally.

©2008 Optical Society of America

**OCIS codes:** (120.3180) Interferometry; (040.2840) Heterodyne; (120.5050) Phase measurement; (120.2130) Ellipsometry and Polarimetry.

## References and links

1. R. M. A. Azzam and N. M. Bashara, *Ellipsometry and Polarized Light* (North-Holland, Amsterdam, 1987).
2. C. H. Lin, C. Chou, and K. S. Chang, "Real time interferometric ellipsometry with optical heterodyne and phase lock-in techniques," *Appl. Opt.* **29**, 5159–5162 (1990).
3. R. E. Ziemer and W. H. Tranter, *Principles of Communications* (Wiley, New York, 1995), Chap. 6.
4. Y. Y. Cheng and J. C. Wyant, "Phase shifter calibration in phase-shifting interferometry," *Appl. Opt.* **24**, 3049–3052 (1985).
5. M. Sato, K. Seino, K. Onodera and N. Tanno, "Phase-drift suppression using harmonics in heterodyne detection and its application to optical coherence tomography," *Opt. Commun.* **184**, 95–104 (2000).
6. P. Yeh and C. Gu, *Optics of Liquid Crystal Displays* (Wiley, New York, 1999), Chap. 5.
7. C. Yang, A. Wax, R. R. Dasari, and M. S. Feld, " $2\pi$  ambiguity-free optical distance measurement with subnanometer precision with a novel phase-crossing low-coherence interferometer," *Opt. Lett.* **27**, 77–79 (2002).
8. T. E. Jenkins, "Multiple-angle-of-incidence ellipsometry," *J. Phys. D. Appl. Phys.* **32**, R45–R56 (1999).
9. K. Riedling, *Ellipsometry for Industrial Applications* (Springer-Verlag, New York, 1988).
10. L. R. Watkins and M. D. Hoogerland, "Interferometric ellipsometer with wavelength-modulated laser diode source," *Appl. Opt.* **43**, 4362–4366 (2004).
11. C. Chou, C. W. Lyu, and L. C. Peng, "Polarized differential phase laser scanning microscope," *Appl. Opt.* **40**, 95–99 (2001).
12. C. Chou, H. K. Teng, C. C. Tsai, and L. P. Yu, "Balanced detector interferometric ellipsometer," *J. Opt. Soc. Am. A* **23**, 2871–2879 (2006).
13. Y. Q. Li, D. Guzun, and M. Xiao, "Sub-shot-noise-limited optical heterodyne detection using an amplitude-squeezed local oscillator," *Phys. Rev. Lett.* **82**, 5225–5228 (1999).
14. C. Chou, Y. C. Huang, and M. Chang, "Effect of elliptical birefringence on the measurement of the phase retardation of a quartz wave plate by an optical heterodyne polarimeter," *J. Opt. Soc. Am. A* **14**, 1367–1372 (1997).
15. C. C. Tsai, H. C. Wei, C. H. Hsieh, L. P. Yu, C. R. Yu, H. S. Huang, and C. Chou, "Characterization of a nematic PALC at large oblique incidence angle," *Opt. Express* **15**, 10381–10389 (2007).

## 1. Introduction

Theoretically, the elliptical polarization can be completely determined by means of the ellipsometric parameters (EP). They are the phase retardation  $\Delta$ , between two orthogonal linear P and S polarized waves and the arc-tangent of the ratio of amplitudes  $\psi$ , of P and S waves produced by specimen. Experimentally, the measuring speeds of  $\Delta$  and  $\psi$  are important to the ellipsometer if the specimen is required to be measured in real time. However, the limited decoding speed on phase detection via phase lock loop analogically [1, 2] results in limited measuring speed on EP measurement. In conventional method, the fast phase decoding method is based on digital technique in temporal domain. However, the decoding phase error and speed are trade-off and critical to the sampling rate of the phase signal [3]. In contrast, the phase detection in spatial domain such as phase-shifting interferometer (PSI) is focused on fringe pattern analysis numerically [4]. Thus, several steps of precise displacement of the reference mirror are required in order to record a number of intensity images accordingly. Therefore, the error on phase shift in reference channel becomes critical to the recovered phase image. As a result, the position error of the reference mirror causes systematic error on surface profile measurement in PSI [5]. In this research, an amplitude-sensitive differential-phase decoding method is proposed in which a common path polarized heterodyne interferometer integrated with a novel balanced detector is constructed able to become a high speed interferometric ellipsometer (HSIE). Then, high sensitivity and fast responding ability on EP measurement by HSIE via conventional envelope detection technique are analyzed and discussed. Three channels of polarized heterodyne signals are recorded simultaneously in HSIE in order to avoid the requirement of equal amplitude of P and S polarized heterodyne signals from tested surface for  $(\Delta, \psi)$  measurements. In addition, HSIE is able to measure EP in real time too. In order to verify the principle of HSIE experimentally, a quarter wave plate (QWP) and a liquid crystal device (LCD) were tested whereas, the dynamic range on differential-phase detection within  $0^\circ$  and  $180^\circ$  was measurable. In the mean time, the frequency response on linear birefringence of anisotropic material, such as LCD, can use HSIE to characterize the optical properties of LCD dynamically [6] for checking better quality display image. Similarly, HSIE is able to measure biological membranes dynamics in life sciences too [7]. Conventionally, to measure phase change relying on lock-in amplifier is the mostly popular method for this purpose. However, slow measuring speed and limited phase detection sensitivity do not satisfy the requirement of real time EP measurement of specimen recently. The conventional photometric ellipsometer (PE) in which the phase and amplitude of the emerging intensity-modulated laser beam are able to be detected simultaneously that EP is obtained in real time. However, the excess noise of laser intensity degrades the sensitivity of detection apparently. Besides, a limited dynamic range is resulted too [1,8,9]. Thus, a method able to measure the phase change at high speed and high sensitivity become urgently requested for various applications [1,9]. Recently, Watkins, *et al.*, [10] proposed a wavelength-modulated laser diode interferometric ellipsometer based on Michelson interferometer. However, the wavelength-dependent optical component and the instability of the wavelength shift due to temperature effect caused the uncertainty of EP measurement apparently. Chou, *et al.*, [11] proposed a differential-phase laser scanning microscope that is able to decode the differential- phase at high sensitivity and in real time by integrating a novel balanced detector in a polarized common-path heterodyne interferometer where the balanced detection can effectively eliminate the excess noise of laser intensity fluctuation obviously [12,13]. However, equal amplitude of two polarized heterodyne signals is required such that the dependence on reflectivity and absorption of the specimen for scanning surface profile limits the applicability in their method. In order to extend this method able to measure EP with various specimens at high speed, we propose HSIE not only able to measure EP in real time but also to relax the requirement of equal amplitude of two polarized

heterodyne signals. In addition, high detection sensitivity is applicable too by use of HSIE based on amplitude-sensitive detection technique. In the context, the working principle of HSIE is derived in section 2. The experimental setup and the results on testing a QWP and a parallel aligned liquid crystal device (PALCD) were tested in order to verify the working principle of HSIE. Moreover, the analogical phase modulation to amplitude modulation conversion HSIE is analyzed and discussed. Not only high detection sensitivity but also high responding ability on EP measurement by using HSIE is demonstrated. Furthermore, a common phase noise rejection mode is provided in HSIE too in which the insensitivity on environmental disturbance of phase detection is discussed.

## 2. Methodology and experimental setup

The optical setup is shown in Fig. 1. It is based on the configuration of our previously developed system on differential-phase detection by use of amplitude-sensitive measurement [11, 12]. A frequency-stabilized linearly polarized laser beam is used in this polarized common-path heterodyne interferometer that three heterodyne signals including P polarized heterodyne signal, S polarized heterodyne signal, and also their differential one, are measured simultaneously. All these heterodyne signals are modulated at the same carrier frequency. Among them, the P polarized ( $P_1+P_2$ ) and S polarized ( $S_1+S_2$ ) heterodyne signals are phase-modulated. However, the difference of these two polarized heterodyne signals from a differential amplifier (DA) in the interferometer is converted into an amplitude modulated signal analytically. In previous setup [11], equal amplitude of P and S polarized heterodyne signals is required for phase to amplitude modulation conversion analytically. However, in this novel phase decoding method, unequal amplitudes of P and S polarized signals are acceptable for being able to convert the phase modulation to amplitude modulation analytically. As shown in Fig. 1, two polarizers are inserted into the reference and signal channels separately. They are adjusted at  $45^\circ$  to x-axis in order to generate  $P_1+S_1$  waves in reference channel and  $P_2+S_2$  waves in the signal channel under the conditions of  $A_{p_1} = A_{s_1}$  and  $A_{p_2} = A_{s_2}$  where  $A_{p_1}$ ,  $A_{s_1}$ ,  $A_{p_2}$ , and  $A_{s_2}$  are the amplitudes of  $P_1$ ,  $S_1$ ,  $P_2$ , and  $S_2$  waves, respectively. Then, the polarized heterodyne signals at photo-detectors  $D_p$  and  $D_s$  can be expressed by

$$I_p(\delta\omega t) = A_{p_1}^2 + A_{p_2}^2 + 2A_{p_1}A_{p_2} \cos[\delta\omega t + \delta\phi_p], \quad (1)$$

$$I_s(\delta\omega t) = A_{s_1}^2 + A_{s_2}^2 + 2A_{s_1}A_{s_2} \cos[\delta\omega t + \delta\phi_s], \quad (2)$$

where  $\delta\phi_p = \phi_{p_1} - \phi_{p_2}$  and  $\delta\phi_s = \phi_{s_1} - \phi_{s_2}$  are the phase retardations between  $P_1$  and  $P_2$  waves and between  $S_1$  and  $S_2$  waves respectively. The beat frequency of the heterodyne signal is  $\delta\omega = \omega_1 - \omega_2$  where  $\omega_1$  and  $\omega_2$  are the driving frequencies of acousto-optic modulators in the reference and the signal arms. If only AC terms are considered, Eqs. (1) and (2) become

$$I_p(\delta\omega t) = 2A_{p_1}A_{p_2} \cos[\delta\omega t + \delta\phi_p], \quad (3)$$

$$I_s(\delta\omega t) = 2A_{s_1}A_{s_2} \cos[\delta\omega t + \delta\phi_s], \quad (4)$$

where no specimen is inserted into the signal channel.  $I_p(\delta\omega t)$  and  $I_s(\delta\omega t)$  is under the conditions of  $\Delta \equiv \delta\phi_s - \delta\phi_p \equiv 0^\circ$  and  $\psi \equiv \tan^{-1}(A_{s_1}A_{s_2} / A_{p_1}A_{p_2}) = 45^\circ$  because  $\phi_{s_1} = \phi_{p_1}$ ,  $\phi_{s_2} = \phi_{p_2}$ ,  $A_{s_1} = A_{p_1}$ , and  $A_{s_2} = A_{p_2}$  are satisfied at the same time. In contrast, when the specimen is inserted into signal channel for testing, both ellipsometric parameters, the phase difference  $\Delta$  and the arctangent of amplitude ratio  $\psi$  of  $P_2$  and  $S_2$  polarized waves, can be obtained by use of a lock-in amplifier (LIA) properly. However, a slow response of the measurement is resulted because the phase lock-in technique is involved. In order to avoid from using LIA and also able to enhance the time response of the EP measurements, we set

$\alpha = \delta\omega t + \frac{\delta\phi_s + \delta\phi_p}{2}$ ,  $\beta = \frac{\delta\phi_s - \delta\phi_p}{2}$ ,  $\kappa_p = 2A_{p1}A_{p2}$ , and  $\kappa_s = 2A_{s1}A_{s2}$  in Eqs. (3) and (4), then

$$I_p(\delta\omega t) \equiv \kappa_p \cos[\alpha - \beta], \quad (5)$$

$$I_s(\delta\omega t) \equiv \kappa_s \cos[\alpha + \beta], \quad (6)$$

whereas,  $A_{p1} = A_{s1}$  and  $\phi_{p1} = \phi_{s1}$  are satisfied in the reference channel by calibration. Let  $(\kappa_s - \kappa_p) \cos \beta = \cos \gamma$  and  $(\kappa_s + \kappa_p) \sin \beta = \sin \gamma$ , then the output signal  $I_{Diff}(\delta\omega t)$ , from DA in Fig. 1 can be expressed by

$$\begin{aligned} I_{Diff}(\delta\omega t) &= I_s(\delta\omega t) - I_p(\delta\omega t) \\ &= (\kappa_s - \kappa_p) \cos \beta \cos \alpha - (\kappa_s + \kappa_p) \sin \beta \sin \alpha \\ &= \cos \gamma \cos \alpha - \sin \gamma \sin \alpha = \sqrt{\kappa_s^2 + \kappa_p^2 - 2\kappa_s \kappa_p \cos(\delta\phi_s - \delta\phi_p)} \cos(\alpha + \gamma), \quad (7) \\ &= \kappa_{Diff} \cos(\alpha + \gamma) \end{aligned}$$

where  $\kappa_{Diff} = \sqrt{\kappa_s^2 + \kappa_p^2 - 2\kappa_s \kappa_p \cos(\delta\phi_s - \delta\phi_p)}$  and  $\gamma$  is a virtual phase angle related to  $\kappa_p$  and  $\kappa_s$ . The  $\kappa_{Diff}$  is the amplitude of  $I_{Diff}(\delta\omega t)$  which belongs to an amplitude-modulated signal of the beat frequency  $\delta\omega$ . Thus,  $\Delta = \delta\phi_{s2} - \delta\phi_{p2}$  and  $\psi = \tan^{-1}\left(\frac{A_{s2}}{A_{p2}}\right)$  are obtained simultaneously in terms of  $\kappa_p$ ,  $\kappa_s$ , and  $\kappa_{Diff}$  by using conventional envelope detection technique. This is not only able to increase the sensitivity but also to enhance the frequency response at the same time. Thus,

$$\Delta = \cos^{-1}\left[\frac{\kappa_p^2 + \kappa_s^2 - \kappa_{Diff}^2}{2\kappa_p \kappa_s}\right], \quad (8)$$

$$\psi = \tan^{-1}\left(\frac{\kappa_s}{\kappa_p}\right). \quad (9)$$

The EP of specimen are then able to be measured precisely in terms of  $\kappa_s$ ,  $\kappa_p$ , and  $\kappa_{Diff}$  in real time.

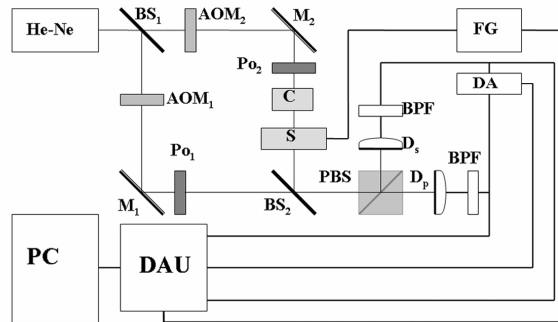


Fig. 1. The optical setup: **He-Ne**: laser source, **BS<sub>1</sub>**, **BS<sub>2</sub>**: beam splitters, **AOM<sub>1</sub>**, **AOM<sub>2</sub>**: acousto-optic modulators, **M<sub>1</sub>**, **M<sub>2</sub>**: mirrors, **Po<sub>1</sub>**, **Po<sub>2</sub>**: polarizers, **C**: compensator, **S**: sample, **PBS**: polarization beam splitter, **D<sub>p</sub>**, **D<sub>s</sub>**: detectors, **BPF**: band-pass filter, **DA**: differential amplifier, **FG**: function generator, **DAU**: data acquisition unit, **PC**: personal computer

### 3. Experimental results

In Fig. 1, two acousto-optic modulators, AOM<sub>1</sub> and AOM<sub>2</sub> were driven at 80.000 MHz and 80.033 MHz respectively as the frequency shifters. Po<sub>1</sub> and Po<sub>2</sub> are polarizers in the reference and signal channels at 45° to x-axis in the interferometer. C is the compensator in order to initialize the zero differential-phase between P and S heterodyne signals from the contribution of optical components. There are three digital voltmeters (DVMs) (Agilent, #34401A) in data acquisition unit (DAU) to record the amplitudes of the heterodyne signals output from D<sub>p</sub>, D<sub>s</sub> and DA (LeCroy, #DA1855A) simultaneously. Then, the parameters  $\psi$  and  $\Delta$  are measured in real-time by use of personal computer. Experimentally, a quarter wave plate (QWP) (CVI, #QWPO-633-10-4) was tested and the experimental results of  $\kappa_s$ ,  $\kappa_p$ , and  $\kappa_{Diff}$  are shown in Fig. 2(a) where the QWP was rotated along its normal axis during the measurement. It is obvious that  $\kappa_s \neq \kappa_p$  in the measurement. Figure 2(b) shows the response of amplitude ratio of  $(\kappa_s/\kappa_p)$  from the detected heterodyne signals at photo detectors D<sub>p</sub> and D<sub>s</sub> according to Eqs. (3) and (4). The result is identical to our previous result of same experimental setup [14]. Correspondingly, the parameter  $\psi$  is obtained and shown in Fig. 2(c). The noise level in Fig. 2(a) at the rotation angle of near 300° was caused by the instability of the laser. However, the ratio of  $\kappa_s$ , and  $\kappa_p$  in Fig. 2(b) remains the same level on signal to noise ratio apparently. This indicates the high correlation between P and S heterodyne signals as such the noise level can be reduced effectively. In other words, HSIE is able to perform noise resistance compared with conventional photometric ellipsometer. In the mean time, the measured phase retardation  $\Delta$  is shown in Fig. 2(d) where the absolute value of phase retardation was recorded. In order to recover full cycle of the response, a conversion was made numerically as shown in Fig. 2(e). Because of a DC phase bias existing in Fig. 2(e) which was generated by optical components in the interferometer, the phase bias can be compensated by adjusting the compensator C until the DC phase bias becomes 0° as shown in Fig. 2(f). Then the measured  $\Delta$  becomes well agree with the measurement by using a lock-in amplifier (LIA) (solid line). Similarly, the same performance on noise resistance of phase is observed too. From these measured results, the validation of working principle of HSIE based on amplitude-sensitive detection method is demonstrated and proved experimentally.

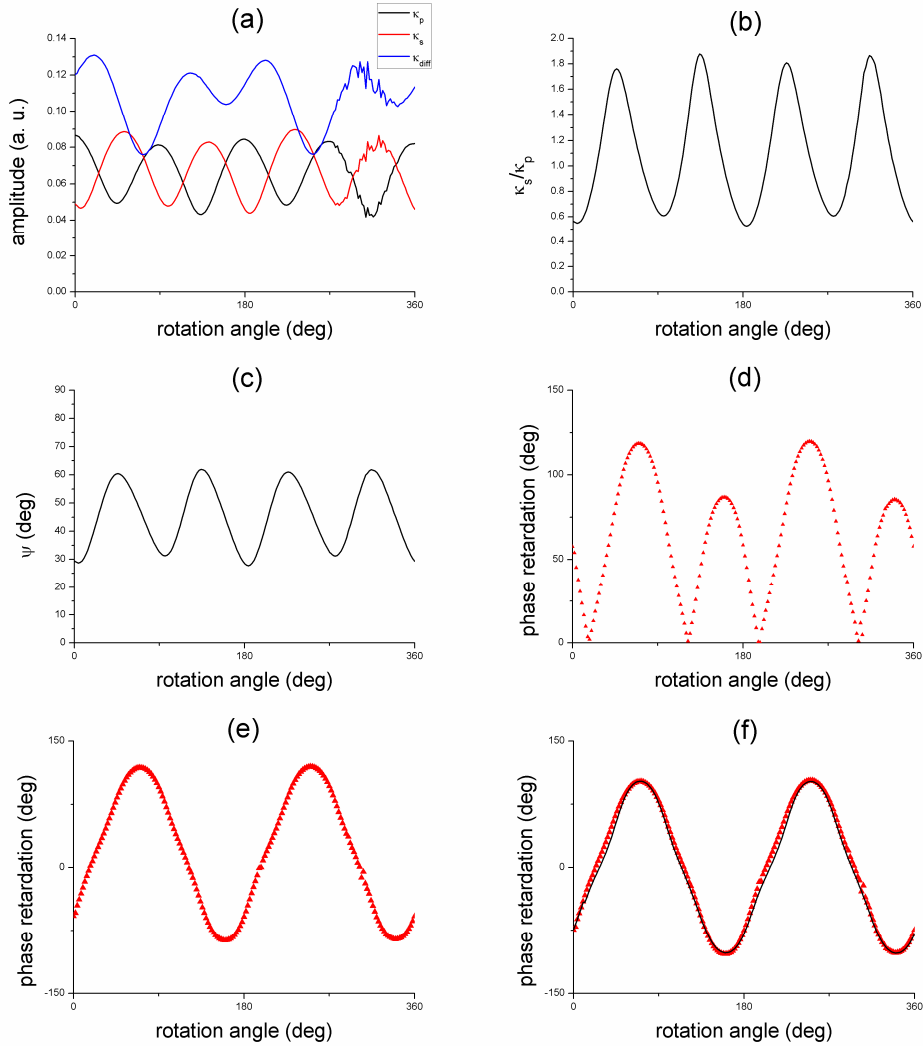


Fig. 2. Experimental results of (a) the amplitudes of P polarized, S polarized heterodyne signals, and their difference, (b) the amplitude ratio of P and S heterodyne signals, (c) the parameter  $\psi$ , (d) the absolute value of phase retardation versus rotation angle of  $180^\circ$  dynamic range, (e) the recovered phase retardation with DC phase bias, (f) the phase retardation of zero DC phase bias is consistent with the experimental curve measured by LIA (solid line).

Meanwhile, in order to check the ability of real time measurement of HSIE, a homogeneous parallel aligned liquid crystal device (PALCD) was tested. It can be measured by measuring time-dependent phase retardation of PALCD which is controlled by an external applied voltage dynamically. Figure 3(a) shows the structure of LC molecule which is equivalent to an index ellipsoid as shown in Fig. 3(b) [15]. The spatial orientation of LC molecule is further defined in Fig. 3(c) in which the incident light is along z-axis. The azimuth angle  $\theta$ , is the angle between the projected direction of LC molecule onto x-y plane and x-axis. In the mean time, the pretilt angle  $\theta_{pre}$ , is the angle between LC molecules and the parallel plane of glass substrate at off-state as shown in Fig. 3(c). When AC voltage is applied, the LC molecules between two Indium-Tin-Oxide (ITO) layers are symmetrically tilted as

shown in Fig. 3(d). The relation of effectively tilted angle  $\theta_{et}$ , can be described by  $n_e(\theta_{et}) = (\int_{z=0}^d n_e(\theta(z))dz) / d$  where  $\theta$  is function of  $z$  and  $d$  is the LC cell gap [6].

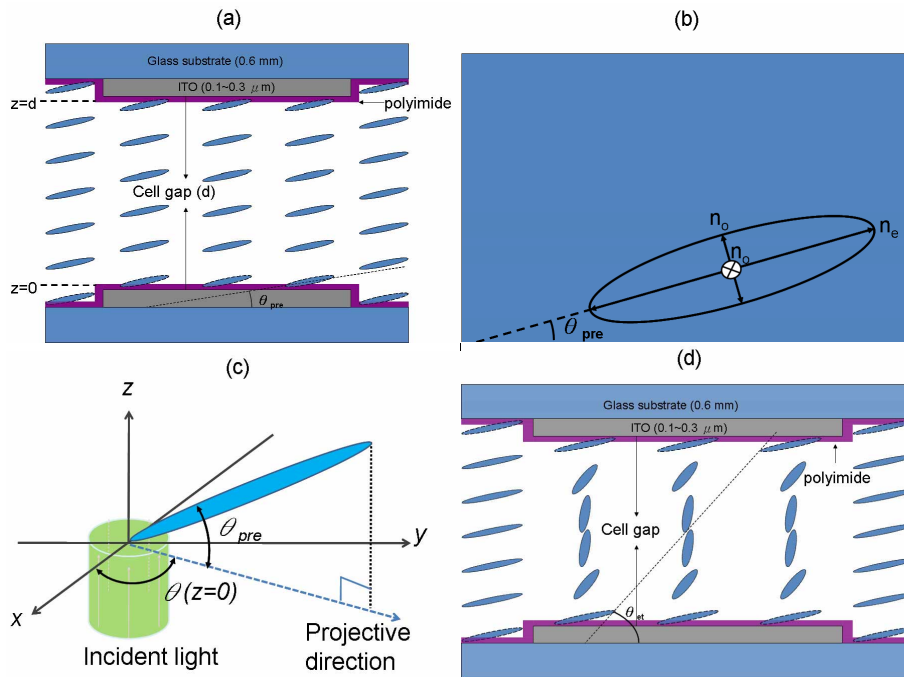


Fig. 3. The molecular alignment of homogeneous LC at (a) parallel-aligned condition at off-state with initial orientation  $\theta_{pre}$ , (b) the effective index ellipsoid model of homogeneous LC, (c) the side view of PALCD in order to find the relation between PALCD and the incident laser beam, (d) symmetrically tilted condition of molecules to the central surface ( $z=d/2$ ) between two ITO films with applied voltage at on-state where the effective tilt angle is  $\theta_{et}$ .

In order to ensure that the mean direction of off-state homogeneous LC molecules are in  $y$ - $z$  plane under the condition of zero voltage applied, PALCD is rotated until the phase retardation is maximized by using LIA in this experiment. And then, the AC voltage is applied by increments until 12 Volts. However, the change of phase retardation as shown in Fig. 4 was out of the dynamic range ( $0^\circ \leq \Delta \leq 180^\circ$ ) measured by LIA. Thus, a suitably adjustment on the azimuth angle  $\theta$  (see Fig. 3(c)) is adjusted until  $\Delta$  of PALCD is within  $0^\circ \leq \Delta \leq 180^\circ$ . Figure 4 shows the response of phase retardation versus applied AC voltage. There is a plateau happened at small applied voltage and then drop rapidly until a smooth response is reached. From the measurement, we can clearly see the non-uniform response of LC molecules to the applied voltage which is similar to the transmission response of TN-LCD [6]. This also can be applied to in-plane-switching (IPS) mode on PALCD [6].

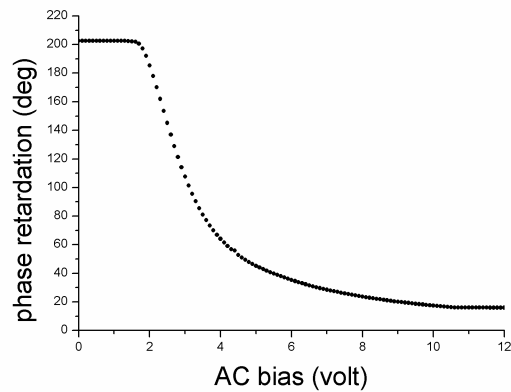


Fig. 4. Experimental results of phase retardation versus AC square-wave voltage (1 KHz) on homogeneous PALCD by slowly increasing the voltage from 0 V to 12 V.

The time response of  $\Delta$  of PALCD versus applied square wave voltage at 1 KHz is shown in Fig. 5. It is obviously seen that the rise time and decay time are different and can be measured very precisely and dynamically. In this experiment,  $\tau_{\text{rise}} = 186$  ms and  $\tau_{\text{decay}} = 213$  ms were measured. This result proves that the ability of HSIE on high speed  $\Delta$  measurement is applicable. Experimentally, the frequency response of  $\Delta$  is limited by the frequency response of DVM in DAU shown in Fig. 1. The sampling rate was 500 (point/sec) in this experiment. Besides, the repeatability on phase retardation measurement at high speed was tested too.

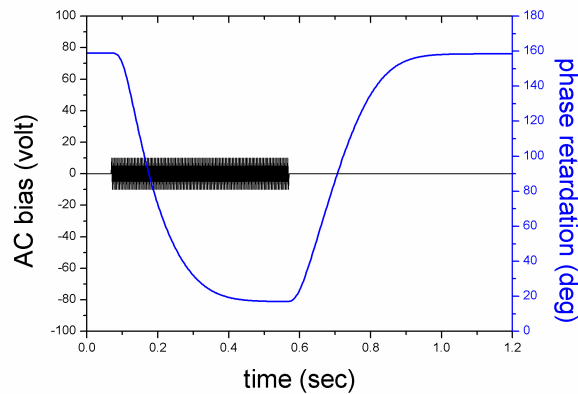


Fig. 5. The rise time  $\tau_{\text{rise}}$  and decay time  $\tau_{\text{decay}}$  of phase retardation of homogeneous PALC under the condition of applying 10 VAC square-wave voltage (1 KHz). In this experiment,  $\tau_{\text{rise}} = 186$  ms and  $\tau_{\text{decay}} = 213$  ms were measured.

The excellent consistence is shown in Fig. 6. This is because of a common-path configuration of HSIE which immunizes the environmental disturbance efficiently. In addition, the novel balanced detector [11] is setup that the excess noise of the laser intensity fluctuation is reduced as well and the shot-noise-limited detection is applicable theoretically [12, 13]. During the measurement, the phase stability of  $\pm 0.01^\circ$  was achieved in this experiment.

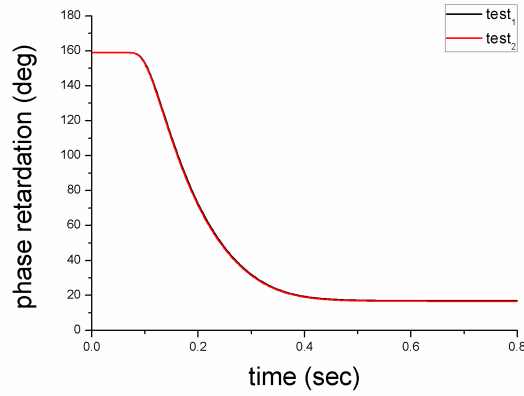


Fig. 6. The repeatable phase retardation measurements of test<sub>1</sub> and test<sub>2</sub> at different time.

#### 4. Error analysis

In order to evaluate the accuracy of this experimental system, the numerical error analyses of the phase retardation  $\Delta$  and the parameter  $\psi$  corresponding to Eqs. (8) and (9) are derived in Eqs. (10) and (11), respectively.

$$\begin{aligned} \delta\Delta &= \left[ \left( \frac{\partial\Delta}{\partial k_p} \right)^2 (\delta k_p)^2 + \left( \frac{\partial\Delta}{\partial k_s} \right)^2 (\delta k_s)^2 + \left( \frac{\partial\Delta}{\partial k_{Diff}} \right)^2 (\delta k_{Diff})^2 \right]^{1/2} \\ &= \left[ \frac{\left( \frac{\kappa_s}{\kappa_p} - \cos\Delta \right)^2 \left( \frac{\delta\kappa_p}{\kappa_p} \right)^2 + \left( \frac{\kappa_p}{\kappa_s} - \cos\Delta \right)^2 \left( \frac{\delta\kappa_s}{\kappa_s} \right)^2 + 2 \left( \frac{\kappa_s}{\kappa_p} + \frac{\kappa_p}{\kappa_s} - \cos\Delta \right)^2 \left( \frac{\delta\kappa_{Diff}}{\kappa_{Diff}} \right)^2}{2(1 - \cos^2\Delta)} \right]^{1/2}. \quad (10) \\ &= \left[ \frac{(\sigma - \cos\Delta)^2 \left( \frac{\delta\kappa_p}{\kappa_p} \right)^2 + \left( \frac{1}{\sigma} - \cos\Delta \right)^2 \left( \frac{\delta\kappa_s}{\kappa_s} \right)^2 + 2 \left( \sigma + \frac{1}{\sigma} - \cos\Delta \right)^2 \left( \frac{\delta\kappa_{Diff}}{\kappa_{Diff}} \right)^2}{2(1 - \cos^2\Delta)} \right]^{1/2} \end{aligned}$$

$$\begin{aligned} \delta\psi &= \left[ \left( \frac{\partial\psi}{\partial k_p} \right)^2 (\delta k_p)^2 + \left( \frac{\partial\psi}{\partial k_s} \right)^2 (\delta k_s)^2 \right]^{1/2} \\ &= \left[ \left( \frac{1}{\frac{k_p}{k_s} + \frac{k_s}{k_p}} \right)^2 \left( \left( \frac{\delta k_p}{k_p} \right)^2 + \left( \frac{\delta k_s}{k_s} \right)^2 \right) \right]^{1/2}. \quad (11) \\ &= \left[ \left( \frac{1}{\frac{1}{\tan^{-1}\psi} + \tan^{-1}\psi} \right)^2 \left( \left( \frac{\delta k_p}{k_p} \right)^2 + \left( \frac{\delta k_s}{k_s} \right)^2 \right) \right]^{1/2} \end{aligned}$$

In Eq. (10),  $\sigma = (\kappa_s / \kappa_p)$  is defined and  $((\delta\kappa_p / \kappa_p), (\delta\kappa_s / \kappa_s), (\delta\kappa_{Diff} / \kappa_{Diff})) = (0.01, 0.01, 0.0025)$  is assumed. The  $(\delta\kappa_p / \kappa_p)$ ,  $(\delta\kappa_s / \kappa_s)$ ,

and  $(\delta\kappa_{Diff}/\kappa_{Diff})$  are defined as  $SNR^{-1}$  of  $\kappa_p$ ,  $\kappa_s$ , and  $\kappa_{Diff}$  respectively which are able to be calculated from Fig. 2(a). Then the phase error  $\delta\Delta$  can be simulated near  $0^\circ$  or  $180^\circ$  for the case of  $\cos\Delta \sim \pm 1.0$  as shown in Figs. 7(a) and 7(b). In Figs. 7(a) and 7(b),  $\delta\Delta$  becomes large when  $\Delta$  is close to  $0^\circ$  or  $180^\circ$  where  $\sigma = 1$ ,  $\sigma = 0.5$ ,  $\sigma = 0.1$  and  $\sigma = 0.01$  are considered. In the experiment of testing QWP in Fig. 2, the error on  $\Delta$  ( $\sim 90^\circ$ ) measurement about  $0.02^\circ$  is seen clearly in Fig. 7(c) in which  $\sigma \sim 0.5$  is assumed from Fig. 2(a). Similarly, to calculate  $\delta\psi$  from Eq. (11), when the  $SNR^{-1}$  is also set at  $(\delta\kappa_p/\kappa_p) \cong (\delta\kappa_s/\kappa_s) = 0.01$ , then  $\delta\psi$  is calculated and shown in Fig. 7(d) in which  $\delta\psi$  is symmetric to  $\psi = 45^\circ$  in the full range of  $0^\circ \leq \psi \leq 90^\circ$ .

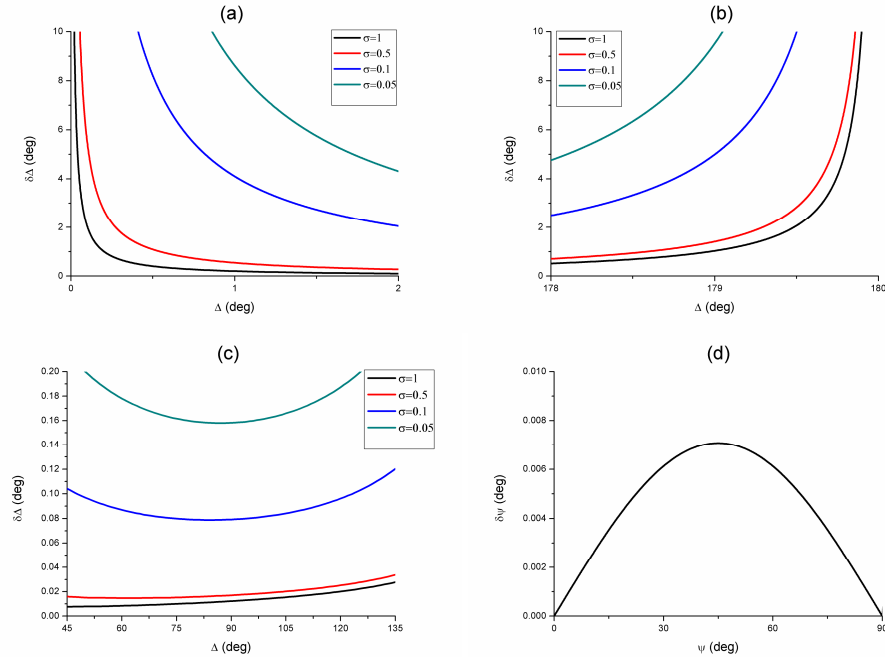


Fig. 7. The error of  $\Delta$  under the conditions of  $(\delta\kappa_p/\kappa_p) = 0.01$ ,  $(\delta\kappa_s/\kappa_s) = 0.01$ , and  $(\delta\kappa_{Diff}/\kappa_{Diff}) = 0.0025$  when (a) the  $\Delta$  is from  $0^\circ$  to  $2^\circ$ , (b) the  $\Delta$  is from  $178^\circ$  to  $180^\circ$ , (c) the  $\Delta$  is from  $45^\circ$  to  $135^\circ$ . The error of  $\psi$  from  $0^\circ$  to  $90^\circ$  is shown in (d).

## 5. Conclusions and discussion

In this study, we proposed and demonstrated a novel amplitude-sensitive interferometric ellipsometer that is able to measure  $(\Delta, \psi)$  of specimen at high sensitivity and in real time. Because of the polarized common-path heterodyne interference in HSIE, the common phase noise rejection mode is provided obviously. Then, high signal to noise ratio (SNR) and modulation index (MI) of the polarized heterodyne signals are generated. Meanwhile, a high correlation between these two polarized heterodyne signals is produced too. Thus, high sensitivity on amplitude-sensitive differential-phase detection is constructed. It is not only able to decode the differential-phase in real time but also can reduce the excess noise of the laser intensity fluctuation. Theoretically, a shot-noise-limited detection is capable in HSIE. In this method, three independent channels of the polarized heterodyne signals are generated and detected at the same time and the requirement of equal amplitude of P and S polarized heterodyne signals becomes unnecessary in HSIE that is applicable on various specimens.

Because the phase retardation  $\Delta$  and the parameter  $\psi$  are in terms of the amplitudes of heterodyne signals, HSIE is not only able to measure EP in real time but also high sensitivity due to the synchronized detection. In addition, a wide dynamic range is anticipated in HSIE too to compare with intensity response in conventional photometric ellipsometer. Both isotropic material and anisotropic material are applicable on measuring EP by using HSIE. This indicates that the reflectivity of surface profile measurement in air or the linear birefringence detection of anisotropic medium are measurable in real time via this novel differential-phase detection method. Besides, this common-path interferometer can reduce the scattering effect as well due to the common-path propagation of highly correlated pair of polarized photons in HSIE [16]. As results, the effect from surface roughness or scattering of specimen is reduced that results in high detection sensitivity in the measurement. Moreover, HSIE can be extended into the areas such as real time monitoring bio-molecular interactions on cell membrane according to the previous analysis. In conclusion, HSIE can measure EP of specimen accurately and in real time by means of amplitude-sensitive detection in a polarized common-path heterodyne interferometer. The common-phase noise rejection mode is provided that results immunity of environmental disturbance effectively. Thus, HSIE improves the performance on fast response and high sensitivity on EP measurements and could become an ellipsometer able to characterize the optical properties of specimen in real time.

### **Acknowledgment**

This research was supported partially by National Science Council of Taiwan through the project NSC-96-2221-E-010-002-MY2.

+C. C. Tsai and H. C. Wei are now with the Graduate Institute of Photonics and Optoelectronics, National Taiwan University, Taipei, Taiwan 106.